PHILOSOPHICAL TRANSACTIONS OF THE ROYAL SOCIETY A MATHEMATICAL, PHYSICAL & ENGINEERING SCIENCES

Models for the growth of rime, glaze, icicles and wet snow on structures

Lasse Makkonen

Phil. Trans. R. Soc. Lond. A 2000 **358**, 2913-2939
doi: 10.1098/rsta.2000.0690

10.1098/rsta.2000.0690

THE ROYAL SOCIETY

Models for the growth of rime, glaze, icicles and wet snow on structures

By Lasse Makkonen

VTT Building Technology, Technical Research Centre of Finland (VTT), Box 18071, 02044 VTT, Finland

Ice accretion on structures is discussed with an emphasis on estimating structural design iceloads and solving operational icing problems. Basic principles of modelling of icing caused by freezing precipitation, cloud droplets and wet snow, as well as simulation of icicle growth, are presented. Theoretical models of atmospheric ice accretion are critically reviewed, particularly with respect to the simulation of the relevant physical processes. The reasons for the difficulties in simulating some icing phenomena accurately are analysed and proposals for further improvements in the models are made.

Keywords: ice; ice accretion; structures; icing; icicles; modelling

1. Introduction

In January 1998 a devastating icing event took place in southern Quebec and eastern Ontario in Canada. Over two million people were without electricity for weeks as 1300 high voltage power-line towers and 35 000 distribution-line towers were destroyed by excessive iceloads. There were 25 deaths and the total damage costs amounted to billions of dollars. The episode not only showed how vulnerable modern societies are to atmospheric icing, but also how difficult it is to predict its magnitude. Ironically, this unexpectedly severe ice storm took place in the only region of the world where regular icing measurements have been made over a long period of time by a dense observation network (Laflamme & Periard 1996). This demonstrates the limitations of direct icing measurements in determining iceloads for structural design.

Extreme icing events are rare results of complex combinations of various atmospheric and geographic factors, and may not follow an occurrence probability distribution that is readily derivable from measured ice data. Also, such data do not exist in most areas of the world. Furthermore, ice data high above the ground, for example for television- and communication-tower design, cannot usually be collected until the tower has been erected. By then it may be too late, as shown by the 140 ice-induced distribution tower collapses in the last 40 years in the US alone (Mulherin 1998).

All this signifies the importance of modelling ice accretion. The major advantages of modelling are that climatic weather data, much more extensive both in time and space than ice data, can be used, and that using sound theoretical model simulations can be extended outside the range of our limited empirical verifications. The latter advantage is particularly important in structural design because the designer is always interested in extreme events that we may not yet have experienced.

Phil. Trans. R. Soc. Lond. A (2000) **358**, 2913–2939

PHILOSOPHICAL TRANSACTIONS OF THE ROYAL SOCIETY A MATHEMATICAL, PHYSICAL & ENGINEERING SCIENCES

Figure 1. Rime on a 22 kV overhead line in Voss, Norway, 18 April 1961. This event is the highest iceload recorded on power lines in the world: 305 kg m^{-1} on each span (photograph from Olav Wist).

Theoretical icing modelling is also required in developing anti-icing and de-icing systems. These are necessary to protect those applications whose safe operation critically depends on even small amounts of accreted ice, due to its effect on their aerodynamic behaviour. These include aeroplanes, helicopters and wind turbines. Aircraft icing modelling has a long tradition (see Gent *et al.*, this issue), while increasing wind-energy production in cold hilly regions of the world has only recently created a demand for anti-icing of wind turbines.

The purpose of this paper is to present a general overview of modelling of atmospheric icing. The emphasis is on icing of ground-based structures, while the theory is to some extent also applicable to icing in air and at sea. This review tries to provide a description of icing modelling mainly from the point of view of the physics. Accordingly, purely statistical models are not reviewed and the discussion does not go deeply into mathematical or numerical methods. Such approaches can be found in the individual papers referred to and in Dranevic (1971), Gartzman (1987) and Poots (1996).

Atmospheric icing occurs in various forms and is due to many physical processes, as discussed in this review. A reader interested in the subject, but having less experience with it, may find it useful to adopt a visual image of the ice deposits whose growth this paper tries to describe theoretically. As a part of the introduction, photographs (figures 1–4) of the basic forms of atmospheric ice are presented to provide food for thought.

2. Fundamentals of icing modelling

The source of natural ice that forms on structures may be either cloud droplets, raindrops, snow or water vapour. In this classification, the term 'cloud droplets'

PHILOSOPHICAL TRANSACTIONS OF THE ROYAL SOCIETY A MATHEMATICAL, PHYSICAL & ENGINEERING SCIENCES

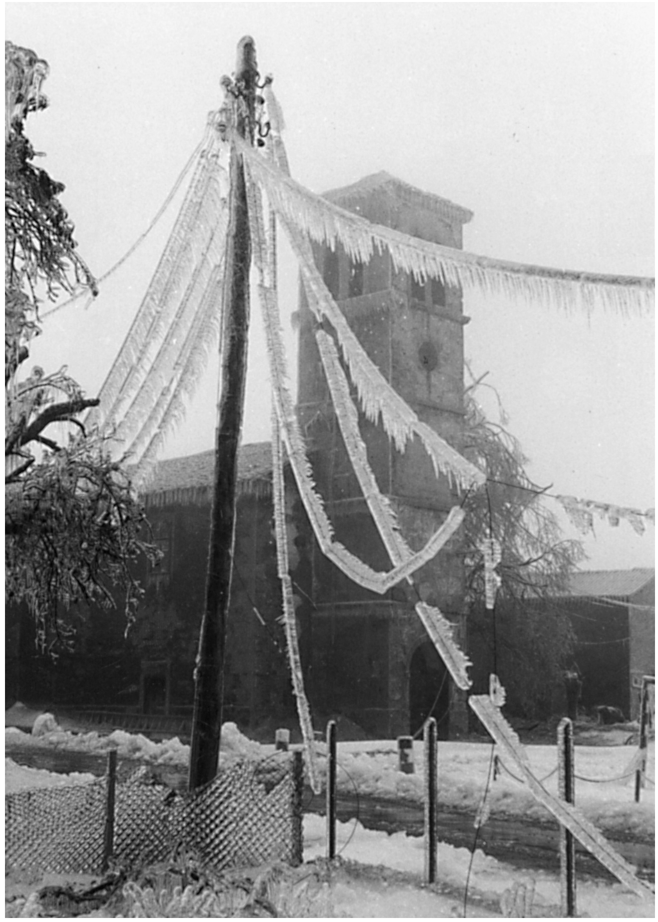

Figure 2. Ice on aerial cables after a freezing-rain event in Slovenia (photograph from IBE, Ljubljana).

includes droplets in clouds that are locally observed as fog, and is separated from 'raindrops' by considerably smaller drop size and, essentially, lower fall velocity. It can be shown (Makkonen 1984*a*) that condensation of water vapour (hoar frost) is usually negligible compared with typical growth rates of ice due to impingement of liquid water droplets and snow particles.

Thus, significant iceloads form due to particles in the air colliding with the object. These particles can be either liquid, solid or a mixture of water and ice. In any case, the maximum rate of icing per unit projection area of the object is determined by the flux density of these particles. The flux density, F, is a product of the mass concentration, w, and the velocity, v, of the particles relative to the object. Consequently, the rate of icing is obtained from

$$\frac{\mathrm{d}M}{\mathrm{d}t} = \alpha_1 \alpha_2 \alpha_3 w \boldsymbol{v} A, \tag{2.1}$$

where A is the cross-sectional area of the object (relative to the direction of the particle velocity vector $\boldsymbol{v}$). The correction factors α_1, α_2 and α_3 represent different

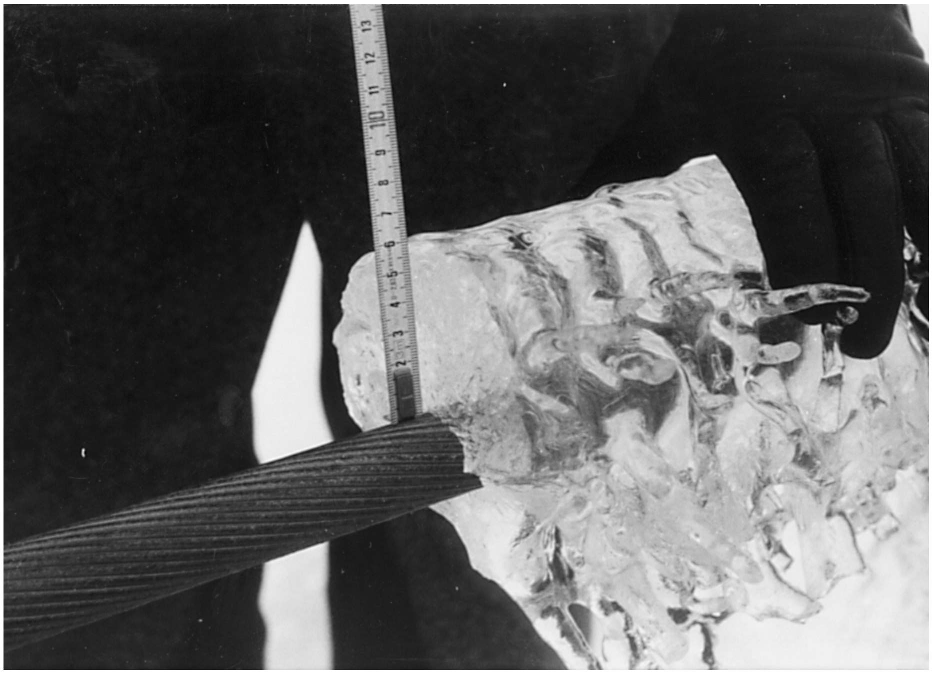

Figure 3. Glaze ice sample taken after the same freezing-rain event as shown in figure 2. The icicles have been partly broken (photograph from IBE, Ljubljana).

processes that may reduce $\mathrm{d}M/\mathrm{d}t$ from its maximum value. The correction factors vary between 0 and 1.

In equation (2.1) α_1 denotes the collision efficiency, α_2 the sticking efficiency, and α_3 the accretion efficiency.

Factor α_1 represents the efficiency of collision of the particles, i.e. α_1 is the ratio of the flux density of the particles that hit the object to the maximum flux density. The collision efficiency α_1 is reduced from unity, because small particles tend to follow the air streamlines and may be deflected from their path towards the object (as shown in figure 5).

Factor α_2 represents the efficiency of collection of those particles that hit the object, i.e. α_2 is the ratio of the flux density of the particles that stick to the object to the flux density of the particles that hit the object. The sticking efficiency α_2 is reduced from unity when the particles bounce from the surface. The particles here are considered to stick when they are permanently collected, or their residence time on the surface is sufficient to affect the icing rate due, for example, to exchange of heat with the surface.

Factor α_3 represents the efficiency of accretion, i.e. α_3 is the ratio of the rate of icing to the flux density of the particles that stick to the surface. The accretion efficiency α_3 is reduced from unity when the heat flux from the accretion is too small to cause sufficient freezing to incorporate all the sticking particles into the accretion. In such a case, part of the mass flux of the particles is lost from the surface by run-off.

When there is no liquid layer and no run-off ($\alpha_3 = 1$) the process is called 'dry growth'. This situation is shown schematically in figure 6. The ice resulting from dry growth is called 'rime'. When the situation shown in figure 7 develops ($\alpha_3 < 1$) there

Figure 4. Wet-snow accretion on a 300 kV power line in Dale-Fana, Norway (photograph from Satnett).

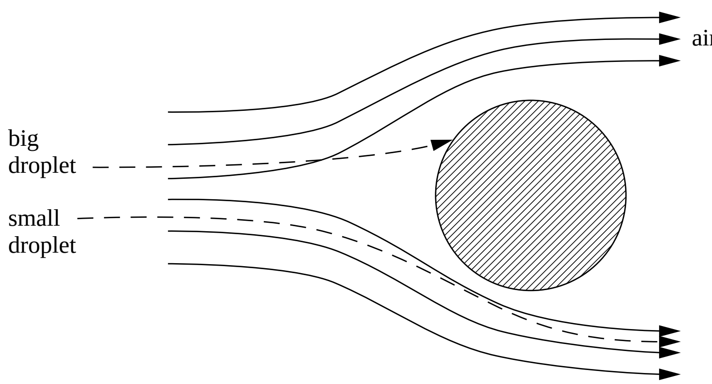

Figure 5. Air streamlines and droplet trajectories around a cylindrical object.

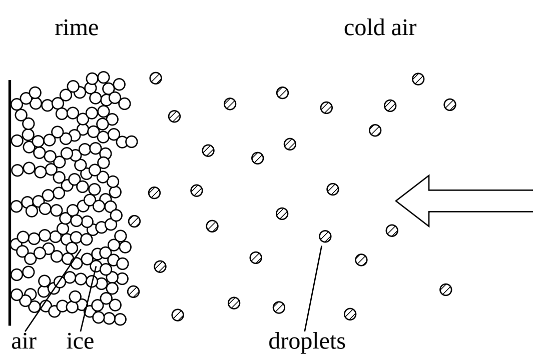

Figure 6. Growth of rime ice (dry growth).

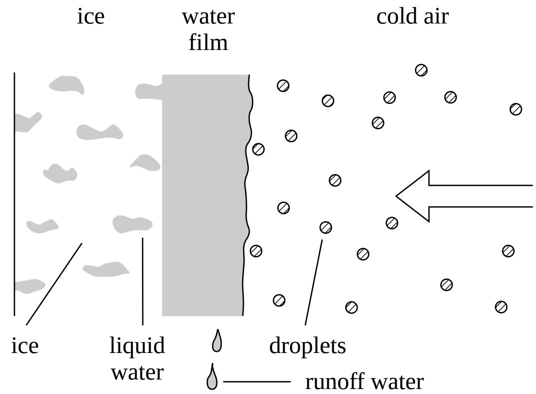

Figure 7. Growth of glaze ice (wet growth).

is a liquid layer on the surface of the accretion and freezing takes place beneath this layer. This is called 'wet growth'. The ice resulting from this process is customarily called 'glaze'. The term 'collection efficiency' for α_1 and the term 'freezing fraction' for α_3 are sometimes used in the literature.

One should note that, although we speak of 'icing' and 'icing rate', $\mathrm{d}M/\mathrm{d}t$, the accretion that forms may be a mixture of ice and liquid water (Macklin 1961). In fact, when a liquid film forms at the accretion surface (figure 7), the growing ice always initially entraps a considerable amount of liquid water (Knight 1968; Makkonen 1987). Accretion of wet snow and growth of icicles (Makkonen 1988) also result in deposits that include liquid water. Liquid water within the accretions is, however, seldom detected, because the deposits often freeze completely soon after the icing storm is over.

As to the estimation of iceloads, one should note that an important, often the most important, parameter is the duration of the icing event. Thus, in addition to the parameters that determine the rate of icing, the key element of successful icing modelling is a good understanding of the combinations during which icing takes place. This is not a trivial problem, but, in short, for freezing precipitation one must account for situations in which the wet bulb temperature is less than 0 °C and there is liquid precipitation; for rime situations where the air temperature is less than 0 °C and there is fog or the location of interest is at a higher altitude than the cloud base; and for wet-snow situations with heavy snow fall when the wet-bulb temperature is greater than 0 °C. Simulation of ice accretion for practical purposes requires careful consideration of all these criteria (Sundin & Makkonen 1998).

3. The rate of icing

Equation (2.1) points out the basic problems of estimating icing rates on structures. Three factors, α_1, α_2 and α_3, which all may vary between 0 and 1, must be determined. In addition, the mass concentration of particles in air, w, the particle velocity, v, and the cross-sectional area of the object, A, must be known. Determination of the atmospheric parameters for a location of interest is more a practical problem than a theoretical one, and will not be discussed here. It may be noted, however, that the mass concentration, w, is not a routinely measured parameter and that its estimation is a difficult problem in its own right, and that the velocity, $\boldsymbol{v}$, is a vector sum of the wind speed and the, often unknown, terminal velocity of the particles.

The complexity of the icing processes (see also figure 8) means that there is little hope of being able to make reasonable predictions of its rate by any simple empirical methods. However, a number of attempts to do this have been made. To a present-day modeller some of these may appear primitive. Nevertheless, one must acknowledge the necessity of extreme design iceload estimates that existed long before our present understanding of the icing physics, not to mention the modern numerical methods. Besides, due to the lack of data on the relevant input parameters, much empiricism must still be included in the modelling, as will become apparent in this review.

The classical empirical approach to estimate the rate of rime icing ($\alpha_2 = \alpha_3 = 1$) is to apply equation (2.1) so that $\alpha_{1\mathrm{w}}A =$ const., i.e. the icing rate depends on the wind speed only. Constants for this equation have been empirically determined by Makkonen (1984*a*) based on data from Rink (1938), Waibel (1955), Baranowski & Liebersbach (1977) and Ahti & Makkonen (1982). As one would expect, these vary with location and provide a poor correlation coefficient. Similar nonlinear equations have also been proposed (Diem 1956), but these also have little predictive value for the reasons that will become evident from the following discussion on the theoretical means of determining the factors α_1, α_2, α_3 and A. Furthermore, as errors in the icing rate tend to average each other out in long-term events, an empirical approach of this kind has some validity in predicting cumulative iceloads, as shown, for example, by Zavarina *et al*. (1976) and Sundin & Makkonen (1998).

Attempts to empirically estimate glaze icing due to freezing rain have generally been made by using the amount of precipitation as the predictor (see, for example, Lenhard 1955). More recent studies have shown, however, that the correlation between the precipitation amount and iceload is very weak (McKay & Thompson 1969; Snitkovskii 1977), so clearly modelling based on the physics is required. As for wet snow, the empirical methods are currently employed and form the basis of modelling, as discussed in § 3 *b* of this review.

(*a*) *Collision efficiency*

When a droplet moves with the airstream towards the icing object, its trajectory is determined by the forces of aerodynamic drag and inertia. If inertial forces are small, then drag will dominate and the droplets will follow the streamlines of air closely (figure 5). Since air must go around the object, the droplets will, in this case, also tend to do so. The actual impingement rate will then be smaller than the flux density of the spray. For large droplets, on the other hand, inertia will dominate and the droplets will tend to hit the object, without being significantly deflected (figure 5).

The relative magnitude of the inertia and drag on the droplets depends on the droplet size, the velocity of the airstream, and the dimensions of the icing object. When these are known, the collision efficiency α_1 can be determined theoretically by numerically solving the equations of droplet motion in the airflow (see, for example, Lock 1990, pp. 182–186). This approach, pioneered by Langmuir & Blodgett (1946) and Mazin (1957), involves numerical solution of the airflow and the droplet trajectories. The trajectories must be determined for a number of particle sizes and impact positions obtained in order to finally derive the overall collision efficiency α_1.

These calculations are complicated and computationally costly. Fortunately, there are several means of simplifying the calculation of α_1 for practical applications.

Firstly, if it is assumed that the icing object is cylindrical, there exists an analytical solution for the airflow around the object, and the collision efficiency can be parametrized by two dimensionless parameters,

$$K = \rho_{\mathrm{w}} d^2 / 9\mu D \tag{3.1}$$

and

$$\phi = Re^2 / K, \tag{3.2}$$

where the droplet Reynolds number, Re, based on the free stream velocity, v, is given by

$$Re = \rho_{\mathrm{a}} dv / \mu. \tag{3.3}$$

Here, d is the droplet diameter, D the cylinder diameter, ρ_{w} the water density, μ the absolute viscosity of air, and ρ_{a} the air density.

Finstad *et al*. (1988*b*) have developed the following empirical fit to the numerically calculated data:

$$\alpha_1 = A - 0.028 - C(B - 0.0454), \tag{3.4}$$

where

$$\left.\begin{aligned} A &= 1.066 K^{-0.00616} \exp(-1.103 K^{-0.688}), \\ B &= 3.641 K^{-0.498} \exp(-1.497 K^{-0.694}), \\ C &= 0.00637(\phi - 100)^{0.381}. \end{aligned}\right\} \tag{3.5}$$

Secondly, Finstad *et al*. (1988*c*) have shown that the single parameter, namely the median volume diameter (MVD), may be used in the calculations (as d in equations (3.1) and (3.3)) with good accuracy, without having to calculate α_1 separately for each droplet-size category.

The collision efficiency α_1 depends strongly on the particle size, and for sufficiently large MVD, such as in freezing rain or wet snow, one can estimate that $\alpha_1 = 1$ in most practical applications, unless the structure is extremely big. Therefore, α_1 usually needs to be calculated only when icing is caused by cloud droplets. It is, however, quite feasible to make calculations of the collision efficiency of wet-snow particles by snowflake trajectory simulations (Skelton & Poots 1991).

(*b*) *Sticking efficiency*

When a supercooled water droplet hits an ice surface it rapidly freezes and does not bounce (figure 6). When there is a liquid layer on the surface, the droplet spreads on the surface and again there is no rebounding (figure 7). Small droplets or ice fragments that leave the surface may be created in these processes (List 1977; Choularton *et al*. 1980; Dong & Hallett 1989). Their relative volume is, however, so small that their effect on icing is usually insignificant. Therefore, liquid water droplets can generally be considered not to bounce, i.e. for water droplets $\alpha_2 \approx 1$.

Snow particles, however, bounce very effectively (Wakahama *et al*. 1977). For completely solid particles, i.e. dry snow, the sticking efficiency, α_2, is basically zero.

When there is a liquid layer on the surface of the snow particles, they stick more effectively, so that at small impact speeds and favourable temperature and humidity conditions α_2 is close to unity for wet snow.

There is presently no detailed theory for the sticking efficiency of wet snow. The available approximation methods of α_2 are empirical equations based on laboratory simulations and some field observations (see, for example, Sakamoto & Miura 1993; see also Poots 1996). The best first approximation for α_2 for cylindrical shapes is probably (Admirat *et al*. 1988)

$$\alpha_2 = 1/v, \tag{3.6}$$

where the wind speed, v, is in $\mathrm{m\,s^{-1}}$. When $v < 1\ \mathrm{m\,s^{-1}}$, $\alpha_2 = 1$.

Air temperature and humidity also affect α_2, but there are presently not enough consistent data to take them into account, despite several experimental studies on this problem (see Poots 1996, pp. 70–72). However, as pointed out above, $\alpha_2 > 0$ only when the snow particle surface is wet, so that snow does not accrete effectively when the wet-bulb temperature is below $0\,^{\circ}\mathrm{C}$ (Makkonen 1989). This criterion is very important because it allows determination of the duration of wet-snow events by climatic weather data.

(*c*) *Accretion efficiency*

In dry-growth icing (figure 6), all the impinging water droplets freeze and the accretion efficiency $\alpha_3 = 1$. In wet-growth icing (figure 7), the freezing rate is controlled by the rate at which the latent heat released in the freezing process can be transferred away from the freezing surface. Then the portion of the impinging water that cannot be frozen runs off the surface due to gravity or wind drag. Simplified approaches to the heat balance of the icing surface have been used in early glaze-ice modelling (see, for example, Imai 1953; Kuroiwa 1965), but we will consider the complete balance here.

The heat balance on the icing surface can, for wet-growth icing, be written as

$$Q_\mathrm{f} + Q_\mathrm{v} = Q_\mathrm{c} + Q_\mathrm{e} + Q_\mathrm{l} + Q_\mathrm{s}, \tag{3.7}$$

where Q_f is the latent heat released during freezing, Q_v is the frictional heating of air, Q_c is the loss of sensible heat to air, Q_e is the heat loss due to evaporation, Q_l is the heat loss in warming the impinging supercooled water to the freezing temperature, and Q_s is the heat loss due to radiation.

The terms of the heat-balance equation can be parametrized using the meteorological and structural variables.

The heat released in the freezing is transferred from the ice–water interface through the liquid water into the air, and consequently there is a negative temperature gradient ahead of the growing ice. This kind of supercooling results in a dendritic growth morphology, and, consequently, some liquid water is trapped within the spray ice matrix. Since the unfrozen water can be entrapped without releasing any latent heat, the term Q_f in equation (3.7) is

$$Q_\mathrm{f} = (1-\lambda)\alpha_3 F L_\mathrm{f}, \tag{3.8}$$

where λ is the liquid fraction of the accretion, and F is the flux density of water to the surface ($F = \alpha_1\alpha_2 w v$). Attempts to determine the liquid fraction, λ, have been made both theoretically (Makkonen 1987, 1990; Blackmore & Lozowski 1996) and experimentally (Lesins *et al*. 1980; Gates *et al*. 1986; Lock & Foster 1990). These studies suggest that λ is rather insensitive to the growth conditions, and that a value of λ around 0.3 is a reasonable first approximation.

Another important consequence of the existence of spongy ice is that the heat conduction into the ice does not need to be considered in the heat balance, since the mixture of ice and water is at the uniform temperature of 0 °C and, therefore, involves no heat conduction through it.

The kinetic heating of air, Q_{v}, is a relatively small term (except at aircraft speeds), but, since it is easily parametrized by

$$Q_{\mathrm{v}} = hrv^2/(2C_p), \tag{3.9}$$

it is usually included in the heat balance. Kinetic heating of the droplets is insignificant and is ignored. Here, h is the convective heat-transfer coefficient, r is the recovery factor for viscous heating ($r = 0.79$ for a cylinder), v is the wind speed, and C_p is the specific heat of air.

The convective heat transfer is

$$Q_{\mathrm{c}} = h(t_{\mathrm{s}} - t_{\mathrm{a}}), \tag{3.10}$$

where t_{s} is the temperature of the icing surface ($t_{\mathrm{s}} = 0$ °C for pure water), and t_{a} is the air temperature.

The evaporative heat transfer is parametrized as

$$Q_{\mathrm{e}} = h\epsilon L_{\mathrm{e}}(e_{\mathrm{s}} - e_{\mathrm{a}})/(C_p p), \tag{3.11}$$

where ϵ is the ratio of the molecular weights of dry air and water vapour ($\epsilon = 0.622$), L_{e} is the latent heat of vaporization, e_{s} is the saturation water vapour pressure over the accretion surface, e_{a} is the ambient vapour pressure in the airstream, and p is the air pressure. Here, e_{s} is a constant (6.17 mbar) and e_{a} is a function of the temperature and relative humidity of ambient air.

The term Q_{l} is caused by the temperature difference between the impinging droplets and the surface of the icing object.

$$Q_{\mathrm{l}} = FC_{\mathrm{w}}(t_{\mathrm{s}} - t_{\mathrm{d}}), \tag{3.12}$$

where C_{w} is the specific heat of water, and t_{d} is the temperature of the droplets at impact.

For cloud droplets, $t_{\mathrm{d}} = t_{\mathrm{a}}$ can be assumed because of their small terminal velocity. This assumption must usually be made also for supercooled raindrops, although they may not have fully adjusted to the temperature at the surface layer during their fall.

The heat loss due to long-wave radiation may be parametrized as

$$Q_{\mathrm{s}} = \sigma a(t_{\mathrm{s}} - t_{\mathrm{a}}), \tag{3.13}$$

where σ is the Stefan–Boltzmann constant (5.67×10^{-8} W m^{-2} K^{-4}), and a is the radiation linearization constant (8.1×10^7 K^3). This equation only takes into account long-wave radiation and assumes emissivities of unity for both the icing surface and the environment. Short-wave radiation of the Sun is neglected because, in practice, atmospheric icing always occurs in cloudy weather.

PHILOSOPHICAL TRANSACTIONS OF THE ROYAL SOCIETY A MATHEMATICAL, PHYSICAL & ENGINEERING SCIENCES

Using the parametrizations of equations (3.8)–(3.14) in the heat-balance equation (3.7) and solving the accretion efficiency results in the following equation:

$$\alpha_3 = \frac{1}{F(1-\lambda)L_{\mathrm{f}}}\left[(h+6a)(t_{\mathrm{s}}-t_{\mathrm{a}}) + \frac{h\epsilon L_{\mathrm{e}}}{C_p p}(e_{\mathrm{s}}-e_{\mathrm{a}}) - \frac{hrv^2}{2C_p} + FC_{\mathrm{w}}(t_{\mathrm{s}}-t_{\mathrm{d}})\right]. \tag{3.14}$$

So far nothing has been said about determining the convective heat-transfer coefficient h in equations (3.9)–(3.11) and (3.14). There are standard methods to estimate both local and overall h on smooth objects with various sizes and shapes (see, for example, Schlichting 1979). In most wet-growth icing models—starting from the very first ones (Ludlam 1951; Imai 1953; Messinger 1953)—it has been assumed that the heat-transfer coefficient of a cylinder or an airfoil represents the icing objects well enough. However, even assuming a simple shape like that, roughness of the ice surface makes the problem rather complicated. The effect of surface roughness on h has been studied in detail theoretically (Makkonen 1985), and this theory can be used as part of an icing model. On the other hand, those factors that control the roughness of the accreting ice are presently poorly known, so that empirical estimates of the roughness scale parameters must be incorporated into the modelling process.

With an estimate of h, equation (3.14) can be used in determining the accretion efficiency α_3, and thereby the rate of icing in equation (2.1). It should be noted that although equation (3.14) has been written in terms of the water flux density F, it is also basically valid locally on the surface of an icing object. In that case, F represents the direct mass flux plus the runback water from the other sectors of the surface. Here, the mean temperature of the net water flux will be different from the temperature of the droplets in the air. In order to predict not only the overall mass of the accretion, but also its shape and vertical distribution, such aspects of formulating the local heat balance have been included in some of the icing models (see, for example, Lozowski *et al*. 1983, 1987; Szilder *et al*. 1987).

It was noted earlier that a criterion for wet-snow accretion is that the wet-bulb temperature is above 0 °C. Then the direction of the heat flux is that from the air to the snow deposit. Thus, during wet-snow accretion, melting of the snow may occur and this may reduce the accretion rate. The thermal balance required to estimate the accretion efficiency α_3 in such a case may be determined similarly to equation (3.14) (Grenier *et al*. 1986; Admirat & Sakamoto 1988). The problem of α_3 for wet snow is, however, very complex, as the excess melt water may, instead of dripping, be soaked into the snow matrix by capillary forces. The extra water in the snow may destroy the network of interconnected ice grains that holds together the snow structure (Colbeck & Ackley 1983). Therefore, it is likely that the upper temperature limit of wet-snow accretion is set by shedding caused by the collapse of the integrity of the snow deposits rather than by overall melting.

4. Numerical modelling

Solving the icing rate analytically from, say, equations (3.4) and (3.14) is not practical, because equations for the dependence of the specific heats and the saturation water vapour pressure on temperature, as well as the procedure for determining h, are involved. Numerical methods must also be used because icing is a time-dependent process, so that the object dimension (A in equation (2.1)) changes upon icing, and

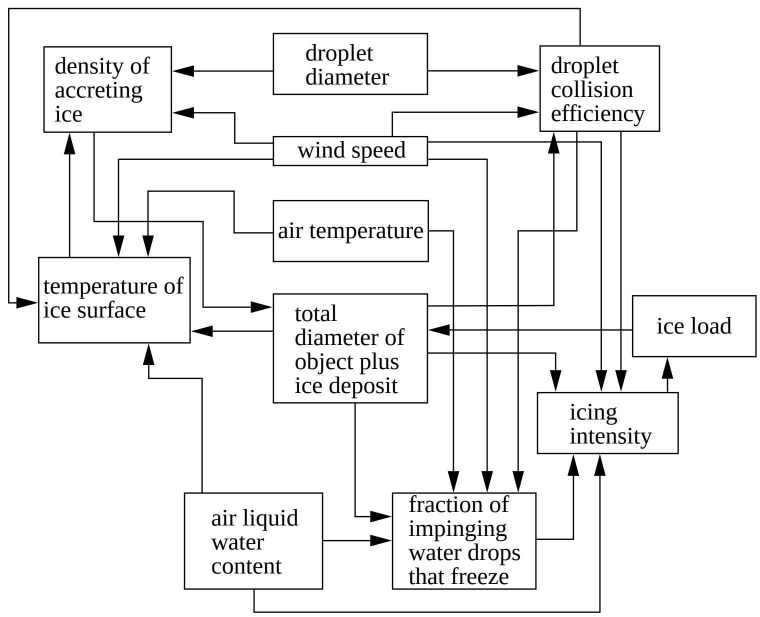

Figure 8. Interdependence of various factors of the icing process caused by water droplets.

this change affects the collision efficiency α_1 and the heat-transfer coefficient h. Furthermore, a change in the deposit dimensions may cause the icing process to transfer from dry growth to wet growth even under constant atmospheric conditions (Makkonen 1984*b*). All this makes the process of icing a rather complicated one. A schematic representation of the many relationships involved is shown in figure 8.

Modern computers provide means of readily obtaining elegant results from the complex icing models (see, for example, Finstad *et al*. 1988*a*). To simplify the modelling, the problem of accretion shape changing with time may be avoided by assuming that the ice deposit maintains its cylindrical geometry. This is a particularly reasonable assumption in the case of rime icing and wet-snow accretion on cables (see Dranevic 1971; also figures 1 and 4).

Time-dependent numerical models of icing also require modelling of the density of the accreted ice. This is because the icing rate for the next time-step depends on the dimensions of the object, and the relationship between the modelled iceload and the dimensions of the iced structure is, therefore, required. It is of historical interest that, prior to the era of numerical models, attempts to simulate rime-ice density were made physically by randomly impacting glued table tennis balls (Buser & Aufdermaur 1973). Nowadays, rime icing can be simulated numerically by ballistic models (Personne & Duroure 1987; Gates *et al*. 1987; Szilder 1993) (as shown in figure 9). Such stochastic models of ice-accretion microstructure have also been expanded into rotating objects (Personne *et al*. 1990) and three-dimensional modelling (Porcu *et al*. 1995; Szilder & Lozowski 1996).

The ballistic modelling approach, where the impinging droplets are supposed to remain spherical at impact, is, however, hampered by the non-spherical shape of natural frozen droplets at high ice-surface temperatures (Macklin & Payne 1968, 1969). The droplet-spreading process is difficult to model, and, therefore, empirical formu-

PHILOSOPHICAL TRANSACTIONS OF THE ROYAL SOCIETY A MATHEMATICAL, PHYSICAL & ENGINEERING SCIENCES

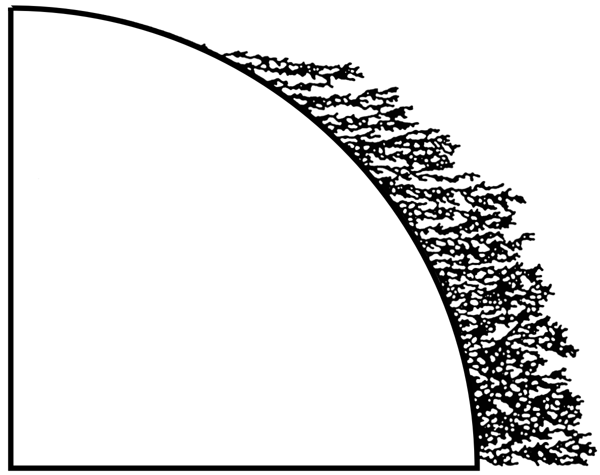

Figure 9. Example of a stochastic ballistic model prediction. Ten-thousand simulated droplets were introduced to produce the simulation (from Gates *et al*. 1987).

lations for rime density are mostly used in rime-icing modelling. Such equations have been proposed by, for example, Macklin (1962), Jones (1990) and Levi *et al*. (1991). For example, the following best-fit equation based on wind-tunnel experiments by Makkonen & Stallabrass (1984) is adequate for the density ρ of rime ice (dry growth) on a slowly rotating cylinder:

$$\rho = 0.378 + 0.425(\log R) - 0.0823(\log R)^2. \tag{4.1}$$

Here, R is Macklin's (1962) parameter:

$$R = -(v_0 d_{\mathrm{m}}/2t_{\mathrm{s}}), \tag{4.2}$$

where v_0 is the droplet impact speed based on the median volume droplet size d_{m}, and t_{s} is the surface temperature of the accretion. Equations to calculate the droplet impact velocity v_0 can be found in Finstad *et al*. (1988*a*). The surface temperature t_{s} must be solved numerically from the heat-balance equation. This can be done by using equation (3.7) and solving equation (3.14) for t_{s} putting $\alpha_1 = 1$. However, because the accretion rate is often too small to release enough latent heat of freezing to significantly heat the icing surface, t_{s} can, in most cases, be approximated by the air temperature t_{a}. For an accurate simulation of the shape of the accretion, rime density may also be calculated locally on the object surface (Bain & Gayet 1983; Finstad & Makkonen 1996).

For glaze ice (wet growth) and icicles the density variations are small and a value of 0.9 g cm^{-3} can be assumed. For wet snow, quantitative estimation of the density is uncertain at present. Some empirical results show that the density of wet snow mainly depends on the air temperature (Sakamoto & Ishihara 1984), while others suggest that it depends on the wind speed (Sakamoto & Miura 1993). Apparently, local climatic conditions play a significant role in these relationships (Admirat *et al*. 1988). Therefore, one usually has to assume a constant empirical value for the wet-snow density, e.g. 0.4 g cm^{-3} (Koshenko & Bashirova 1979), although the scatter is large in natural conditions (Eliasson & Thorsteins 1996).

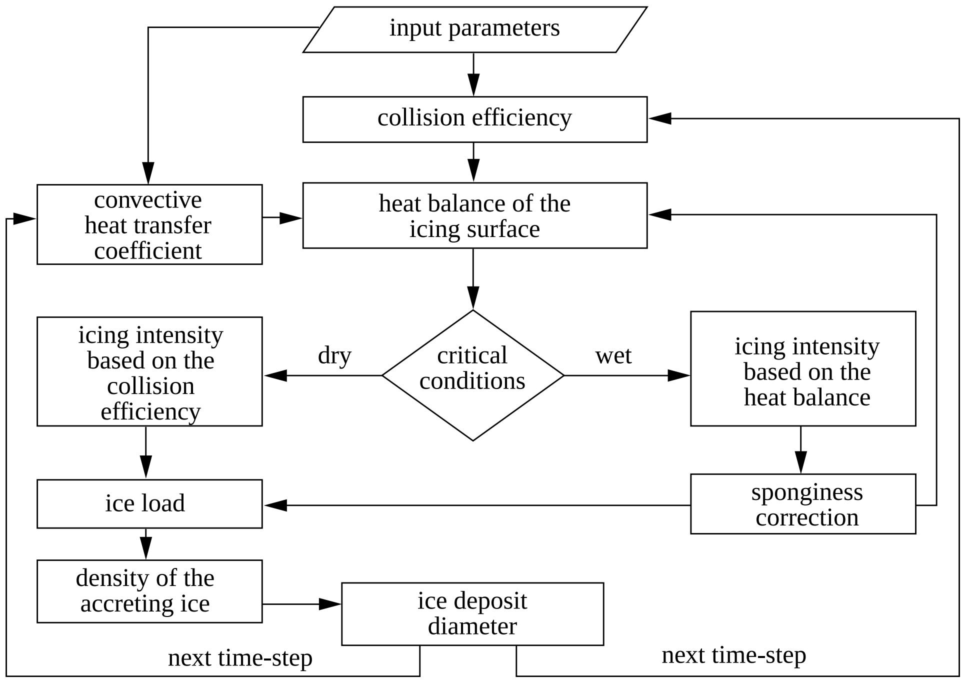

Figure 10. Simplified block-diagram of a numerical icing model.

When the above-mentioned estimates of the density of accretions are included, a numerical model can be developed to simulate time-dependent icing of an object. Various physical phenomena can be included in the model as sub-routines and run selectively according to the input data and the state of the simulated process. Calculation progresses in a stepwise manner. A schematic description of an icing model is shown in figure 10.

A real structure, such as a lattice tower, usually consists of small structural members of different sizes. Modelling of icing of such a complex structure may be done by breaking the structure into an ensemble of smaller elements, calculating the iceload separately for each of them, and finally summing the results to get the total iceload. One may then need to take into account situations where the elements shadow each other or the simulated ice on them grows together forming a single big element.

So far, we have discussed the simulation of the total iceload on an object. Numerical modelling makes it possible to simulate not only the overall collision, accretion and sticking efficiencies of objects, but also their local values along the exposed surfaces. Thus, accretion shape can be simulated. This is of less importance for general iceload estimates, but is very useful in those applications where the aerodynamic forces, as modified by the accreted ice, are significant. These include aircraft wings and wind-turbine blades, as well as aerial cables due to the possibility of aerodynamically induced galloping.

The modelling of the local collision efficiency requires simulation of the airflow over ice-accretion shapes and detailed simulation of droplet trajectories. Several such models (see, for example, Poots & Rodgers 1976; Ackley & Templeton 1979; McComber & Touzot 1981; Scott *et al*. 1987; Jones & Egelhofer 1991; Shin *et al*. 1994; Finstad & Makkonen 1996; Arnold *et al*. 1997) have been developed. Many of them are designed specifically for airfoils and are discussed elsewhere in this issue by Gent *et al*.

The sticking efficiency, relevant for wet-snow accretion modelling, is poorly known in general, and hence its local values must be based on ad hoc assumptions, such as a cosine law (Poots & Skelton 1995). Rather detailed numerical models of wet-snow accretion on power lines have been developed based on such assumptions (see, for example, Skelton & Poots 1991; Poots 1996, 1998), but as long as these models must be based on very rough assumptions of the dependence of α_2 on the atmospheric conditions, the use of such detailed modelling is limited in practice.

The accretion efficiency of wet-growth icing can also be simulated locally using empirical or boundary-layer models for local heat transfer (see, for example, Lozowski *et al*. 1983; MacArthur 1983; Makkonen 1985). A major complication then arises due to the runback water along the surface. Numerical methods to deal with such problems have been developed, particularly for airfoils (see Gent *et al*., this issue) and ships (see Lozowski *et al*., this issue).

Various novel methods, such as stochastic modelling, have also been developed to predict the shape of ice accretions (see, for example, Lozowski *et al*. 1983; Szilder *et al*. 1987; Szilder & Lozowski 1995*a*), but they are of limited use until the factors α_1, α_2 and α_3 in equation (2.1) can be predicted locally for more complex shapes. Nevertheless, these models are a significant step forward, because the shape of the accretion is very important with regard to the wind drag and lift on iced structures.

5. Icicle growth

Icicles are sometimes formed during freezing precipitation (see figures 3 and 4). Previously it was thought that icicles grow only from freezing of the run-off water from the rest of the accretion. Icicles were neglected in ice-accretion modelling and only the overall heat balance of the object was considered in determining the accretion efficiency, or the accretion efficiency was assumed to be unity (Goodwin *et al*. 1983). However, recent numerical simulation of glaze icing in freezing-rain modelling, including icicle growth (Makkonen 1998), has, somewhat surprisingly, shown that when the air temperature is high enough for icicle growth, the total load may be much higher than at any other temperature. Thus, while icicle growth in freezing rain is rarely observed, it is still a relevant factor with regard to the extreme icing events. For these reasons, icicle simulation is now discussed.

When there is a source of water at the root of the icicle, a liquid film forms on the icicle surface and flows towards the tip due to gravity or wind drag. Water spreads effectively on an icicle surface so that liquid water covers the entire icicle surface uniformly, unless the flux of water is extremely small. The thickness of the liquid film on the icicle surface during its growth is typically 40–100 μm (Maeno & Takahashi 1984).

When water flows down along the icicle surface, a part of it freezes, but, if the water supply is sufficient, a pendant drop forms at the tip of the icicle. The pendant drop grows until it reaches a certain size and then falls, whereafter another drop starts to grow. Measurements under calm conditions show that the diameters of the pendant drop and of the tip of the icicle are 4.8–5.0 mm, regardless of growth conditions (Maeno & Takahashi 1984).

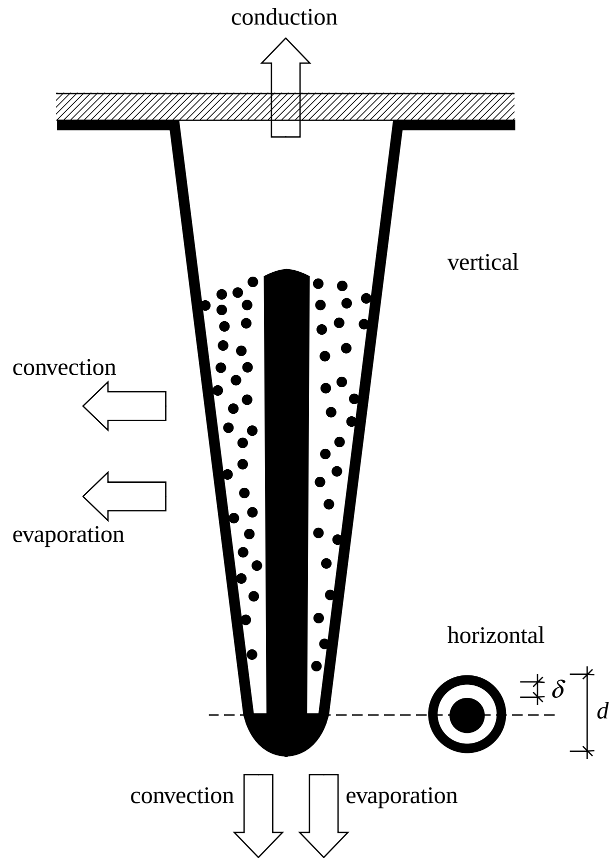

Figure 11. Schematic cross-section of a growing icicle. Dark areas denote liquid water and white areas denote ice. Dimensions are exaggerated.

When an icicle grows, the latent heat of fusion released in the freezing of ice beneath the water film must be removed from the ice–water interface. The rate of heat loss from the surface to the environment, therefore, controls the growth rate of ice. This situation is analogous to 'wet growth'.

The heat loss from the surface to the air is mainly by thermal convection and by evaporation. Outgoing radiation is small and heat conduction in the interior of the icicle is negligible. The pendant drop cools significantly and may therefore release heat to the tip of the icicle.

Makkonen (1988) has shown that, as the observed vertical growth rate of an icicle is much higher than the horizontal growth rate, it is only the vertical dimension of the tip of the icicle that is growing fast, not the mass of ice. In other words, the tip of the icicle grows vertically as a thin cover of ice enclosing unfrozen water. The growing tube of ice within a pendant drop at the icicle tip has a wall thickness of less than 100 μm and depends on the growth rate (Maeno *et al*. 1994). By this mechanism, the surface area from which the heat loss takes place, i.e. the hemispherical surface of the pendant drop, is much bigger than the surface area of the ice that is growing vertically and releasing latent heat of fusion. The situation is shown schematically in figure 11.

The liquid water in the interior of an icicle cannot be frozen by processes that transfer heat downwards or horizontally, because there can be no temperature gradients in these directions, as the walls and the tip of the icicle are at the freezing temperature. Therefore, the only mechanism by which the entrapped liquid water can subsequently be frozen is heat conduction upwards through the root of the icicle. By this process, the liquid water inside the icicle freezes slowly from the root downwards (figure 11). The conduction through the root of the icicle does not affect the icicle growth rate, as it does not contribute to the heat balance of the icicle surface. Only conduction determines how fast the interior of the icicle changes from liquid to solid.

Once the thin cover of ice at the tip of an icicle has grown vertically, it also starts to grow horizontally outwards due to heat loss to the air at the icicle walls. The icicle then grows in width. As the ice on the walls grows beneath a supercooled water film, the ice–water interface assumes a dendritic sub-structure and encloses some liquid water into a spongy ice matrix.

A comprehensive numerical model of icicle growth based on the above physical description has been developed by Makkonen (1988) and further verified by Maeno *et al*. (1994). The model simulations point out that the growth rate of an icicle under constant conditions is strongly time dependent. The elongation rate increases with time under fixed atmospheric conditions and water supply rate. This is mainly due to the decreasing drip rate as more of the supply water is frozen on the walls of the icicle as it gets bigger. The width growth rate slowly decreases with time mainly because the heat-transfer coefficient decreases with increasing icicle diameter. Under fixed conditions, the growth rate of icicle mass increases considerably with time, until the icicle grows so big that there is no drip and no growth in length. By that time all the supply water is collected by the icicle, and the mass-growth rate is constant.

The model results demonstrate that the growth rate of the icicle length decreases with water supply rate, while the growth rate of the icicle width is only slightly affected by it. The net result is that the mass of an icicle decreases with increasing water supply rate, provided that the water supply is constantly sufficient for the icicle to elongate. This result is contrary to what one might intuitively expect, but it is in accordance with data from laboratory tests (Maeno *et al*. 1994). The reason for decreasing elongation rate with increasing water supply is the warming caused by drip water, as the pendant drop leaves the tip more supercooled than when it reaches the tip.

The model suggests no upper limit for the size of an icicle if conditions for its continuous growth prevail. Under natural conditions there are, however, several factors that limit the icicle size. If the water supply rate is high, the icicle initially grows slowly and is unlikely to grow bigger. On the other hand, if it is low, then the icicle soon ceases to elongate due to no water flow to the icicle tip. Very big icicles can, therefore, form only under conditions in which the water supply rate is at first small and then continuously increases. Another limiting factor is that very low air temperatures, favouring rapid icicle growth, seldom occur during freezing rain (Stallabrass 1983). Also, they do not promote the melting of already formed ice or snow accretions above that which might produce the necessary melt water flux for icicles to grow.

The icicle model has been incorporated into a freezing-rain model for a cable (Makkonen 1998) by taking into account the fact that the icicles themselves also collect water droplets directly. This feedback effect is very significant at high wind speeds as it provides the above-mentioned continuous increase in the water supply.

The spacing of icicles, i.e. the number of icicles per unit length of an object, is an important factor in the icing process. Not only is the total load determined by the number of icicles, but also their size depends strongly on the spacing, which controls how much run-off water enters the root of the icicles. The spacing of icicles was solved analytically by Makkonen & Fujii (1993), who also verified the solutions by icing wind-tunnel experiments. Their results, confirmed by a more recent analysis by de Bruyn (1997), show that the spacing of icicles is slightly above 2 cm, regardless of the growth conditions. It is, therefore, not uncommon for big icicles to grow into contact with each other. They may then form a continuous sheet of ice, as can be seen in figure 3.

While the model of Makkonen (1988) is a numerical icicle-simulation algorithm including the fundamental physics, other types of icicle models have also been developed. Szilder & Lozowski (1994) suggest a simple analytical model and Szilder & Lozowski (1995*b*) propose a three-dimensional random-walk model. In the latter model, water flow along the icicle surface is divided into fluid elements that follow a stochastic path towards the icicle tip. During its motion, the element may freeze at positions that have certain given freezing probabilities. Some physics—following the heat-balance approach discussed in § 3 *c*, for example—may then be used to determine these probabilities. The model of Szilder & Lozowski (1995*b*) is particularly interesting, because it is not limited to any specific object geometry (see also Szilder & Lozowski 1995*a*).

6. Discussion

Many fundamental aspects of the state-of-the-art theory of ice accretion on structures have been verified successfully (Macklin & Bailey 1968; Makkonen & Stallabrass 1984, 1987; Gates *et al*. 1986; Maeno *et al*. 1994; Shin *et al*. 1994; Lu *et al*. 1998; Makkonen 1998). However, there remain several uncertain areas that require more verification and development.

There is major uncertainty when the collision efficiency is very small ($\alpha_1 < 0.1$). In such a case the theory tends to predict values of α_1 that are too small (Lehtonen *et al*. 1986; Personne & Gayet 1988; Yano 1988). This may be because the roughness elements of the surface act as individual collectors (Personne *et al*. 1988), due to condensation of water vapour (Makkonen 1992), and due to omission of the history term in the equations of droplet motion (Oleskiw & Lozowski 1983). When α_1 is small the icing rate is also small, so that this problem does not generally hamper the estimation of extreme iceloads for structural design. On the other hand, when the structure is very large (e.g. a fully iced tower, see figure 12), the growth rate of the total iceload may be substantial even at low α_1. Estimates of icing for very large objects, particularly at low wind speeds, should, therefore, be made with caution. There is not much hope of improving the estimation methods in this respect because small values of α_1 are so sensitive to changes in the droplet size that their accurate determination is impossible due to errors in measuring the MVD of the droplets. Thus, empirical methods may also need to be used in the future when estimating rime icing on large objects.

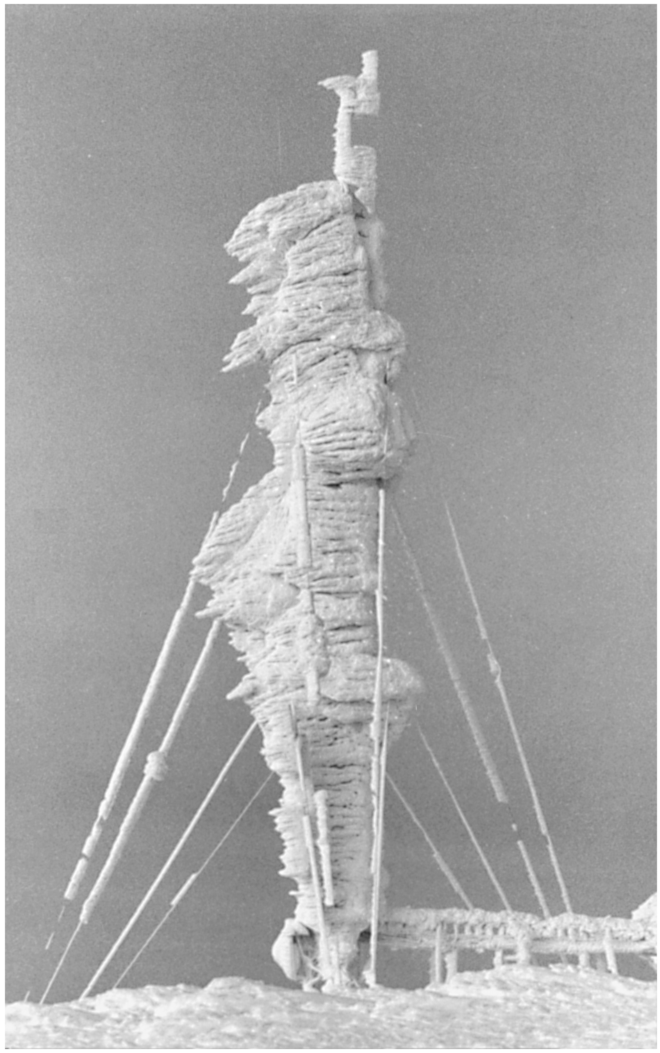

Figure 12. A fully iced lattice communication tower on Ylläs, Finland.

Another relatively poorly known aspect is the effect of droplet trajectory angle on the collision efficiency. This is related to difficulties in modelling the airflow and droplet trajectories around objects with very complex shapes. However, there are also some unsolved problems that are very important to applications which should not be too difficult to model using modern techniques. These include the effect of wind direction with respect to power-line orientation. So far, only very approximate empirical equations are available for estimating this important effect (Nikiforov 1983).

Estimation of the sticking efficiency, α_2, of wet snow is presently quite inaccurate, so that equation (3.6) should be seen only as a first approximation until more sophisticated methods have been developed. Such developments could be based on detailed heat-balance considerations of falling snowflakes following Matsuo & Sasyo (1981). Until then, the theoretical models of wet-snow accretion (Skelton & Poots 1991; see also Poots 1996)—which are otherwise quite sophisticated, but neglect the crucial sticking efficiency problem—cannot be used effectively. In the present situation, simple empirical models (see, for example, Admirat & Sakamoto 1988; Makkonen 1989; Sakamoto & Miura 1993), which at least try to estimate the sticking efficiency, α_2, are preferred.

Theoretical calculation of glaze formation is relatively reliable, provided that the model has the correct input. The weakest part of glaze-ice modelling is presently the lack of data on ice surface roughness for heat-transfer calculations. Further studies should be made on the kinetics on the icing surface along the lines of the studies of Olsen & Walker (1986) and Hansman & Turnock (1988). When icicles may contribute to the iceload, a separate model of icicle growth needs to be incorporated into the modelling, as discussed in this paper. In addition, it is noteworthy that many glaze-icing models presently used for power lines are conceptually suspicious or include other types of error (see Makkonen 1998). Unfortunately, some of these models are still widely used, as parts of national building codes, for example.

Some specific properties of the icing objects may hamper the modelling of iceloads on them. For example, while the diameter (Makkonen 1986) and the torsional stiffness (McComber 1984; Finstad *et al*. 1988*a*; Skelton & Poots 1991; Poots 1996) of a cable can easily be taken into account in the modelling of icing, their effects on ice disappearance cannot. Ice shedding mechanisms related to cable twisting are inadequately understood, considering that they appear to be the primary cause of different iceloads on cables of different torsional properties (Holodov & Popov 1976; Govoni & Ackley 1983). Studying this problem in the future is a challenging task, since there is a strong feedback between ice-accretion growth and twisting of a cable. This is not only because of the aerodynamics of the accretion, but also because the iceload itself initiates torsional motion due to increased cable tension (McComber *et al*. 1995). Further complications regarding icing of power-line cables include the heating effect of an energized cable and the effect of the electric field on droplet trajectories and ice properties (Phan & Laforte 1981; Farzaneh, this issue).

When modelling icing of complex structures, such as lattice towers, some components of the structure may be sheltered from ice accretion by other components. Also, different parts of the structure may completely freeze together, whereafter they should be modelled as a single object. Such aspects must be considered individually for each structure and can also be modelled physically by small-scale icing experiments (Makkonen & Oleskiw 1997).

As to the use of theoretical icing models in predicting design iceloads of structures, the major problem is the input requirement. The median volume droplet size and liquid water content, which are not routinely measured, are less significant when considering atmospheric glaze icing (Makkonen 1981), but critically affect rime icing. Obtaining correct wind velocity data is often uncertain because of the adverse effect of icing on anemometers. Furthermore, rather accurate values of the air temperature and cloud base height are required in order to detect the start and end of the simulated icing episodes correctly (Glukhov 1989; Sundin & Makkonen 1998). Extrapolation of these and other required input parameters to the often-remote sites of interest is extremely difficult. The future usefulness of the theoretical modelling of icing essentially depends on the progress made in this area.

Due to the limitations of theoretical modelling, much emphasis in practical design has to be given to empirical models of icing. Considerable progress in this area has taken place recently, but the success of modelling design loads, which usually form

PHILOSOPHICAL TRANSACTIONS OF THE ROYAL SOCIETY A MATHEMATICAL, PHYSICAL & ENGINEERING SCIENCES

over long time-periods, depends on being able to model the disappearance of ice as well. Field studies (Govoni & Ackley 1983; Lehtonen *et al*. 1986; Sundin & Makkonen 1998) have shown that not only melting but also ice shedding caused by the wind and structure dynamics are important when considering cumulative iceloads. Detailed modelling of these processes has only recently begun (McComber 1990; Scavuzzo *et al*. 1994).

In many cases, the relevant design load of a structure depends on the combination of extreme ice and extreme wind. It is not possible to estimate the probability of combined ice and wind loads over long periods without data on the recurrence of ice. Thus, future safe design of, say, towers, clearly depends on better modelling of ice melting and shedding events. Finally, it is noteworthy that the shedding events themselves may in some cases be more damaging to the structure than the static iceload (Jamaleddine *et al*. 1996; Fekr *et al*. 1998), and that falling ice is always a hazard below. Another key aspect of modelling the combined ice and wind load is the drag coefficient of an iced structure. This aspect should be studied by further experiments (Golikova 1976) and by developing the existing theoretical ideas (McComber & Bouchard 1986).

The main practical significance of the research reviewed in this paper is in estimating extreme iceloads for structural design, and thus promoting safe and economical engineering. Icing data are also required for some operational needs, such as power production estimation for wind turbines in hilly regions. Another ambitious application, already studied preliminarily (see Fuchs *et al*. 1998; Vassbø *et al*. 1998), is to make advanced icing predictions by using numerical mesoscale weather-prediction model results as input. Such forecasts, however, require more specific mesoscale meteorological models to predict the cloud liquid water content and the form of precipitation. These aspects are also presently studied (Reismer *et al*. 1998; Zerr 1997).

A further application of icing theory is in the design and optimization of anti-icing and de-icing equipment and strategies. Such ice-prevention modelling efforts have been made for power line cables, for example, by Grenier *et al*. (1986), and for wind turbines by Marjaniemi & Peltola (1996). These studies, among others, point out the necessity for a deep understanding of the icing processes. Heating a surface may allow relatively dry ice particles to stick, transform the icing process from dry to wet, causing icicle growth, and unfavourably alter the aerodynamics of the ice deposits. De-icing at the wrong moment may cause disastrous dynamic responses from the structure. Overall, poorly designed or uncontrolled ice prevention may not only increase the iceloads, but also initiate icing events that would not otherwise take place and directly cause structural damage.

Modelling of atmospheric ice accretion is motivated throughout the world by a variety of problems that icing causes, but it would not be fair to end this review without also pointing out the usefulness of this fascinating phenomenon. Since accreted ice amounts depend on many atmospheric parameters, it is possible to do icing modelling in a reversed order so that these parameters can be derived from icing measurements. This technique—already put forward by the pioneers of icing modelling (Langmuir & Blodgett 1946) and later developed by Rogers *et al*. (1983), Howe (1991) and Makkonen (1992), for example—now apparently provides more-accurate measurements of the median volume droplet diameter and liquid water content of supercooled clouds than any other method.

References

Ackley, S. F. & Templeton, M. K. 1979 Computer modeling of atmospheric ice accretion. US Army Cold Regions Research and Engineering Laboratory, report 79-4.

Admirat, P. & Sakamoto, Y. 1988 Wet snow on overhead lines: state-of-art. In *Proc. 4th Int. Workshop on Atmospheric Icing of Structures*, pp. 8–13.

Admirat, P., Maccagnan, M. & de Goncourt, B. 1988 Influence of joule effect and of climatic conditions on liquid water content of snow on conductors. In *Proc. 4th Int. Workshop on Atmospheric Icing of Structures*, pp. 367–371.

Ahti, K. & Makkonen, L. 1982 Observations on rime formation in relation to routinely measured meteorological parameters. *Geophysica* **19**, 75–85.

Arnold, K., Tetzlaff, G. & Raabe, A. 1997 Modelling of ice accretion on a non-rotating cylinder. *Meteorol. Z.* **6**, 120–129.

Bain, M. & Gayet, J. F. 1983 Contribution to the modelling of the ice accretion process—ice density variation with the impacted surface angle. *Ann. Glaciol.* **4**, 19–23.

Baranowski, S. & Liebensbach, J. 1977 The intensity of different kinds of rime on the upper tree line in the Sudety mountains. *J. Glaciol.* **19**, 489–497.

Blackmore, R. Z. & Lozowski, E. P. 1996 A freshwater spongy spray icing model with surficial structure. In *Proc. 7th Int. Workshop on Atmospheric Icing of Structures*, pp. 33–43.

Buser, O. & Aufdermaur, A. N. 1973 The density of rime on cylinders. *Q. Jl R. Met. Soc.* **99**, 388–391.

Choularton, T. W., Griggs, D. J., Humood, B. Y. & Lathan, J. 1980 Laboratory studies of riming, and its relation to ice splinter production. *Q. Jl R. Met. Soc.* **106**, 367–374.

Colbeck, S. C. & Ackley, S. F. 1983 Mechanism for ice bonding in wet snow accretions on power lines. In *Proc. 1st Int. Workshop on Atmospheric Icing of Structures*, pp. 25–30.

de Bruyn, J. R. 1997 On the formation of periodic arrays of icicles. *Cold Regions Sci. Technol.* **25**, 225–229.

Diem, M. 1956 Ice loads on high voltage lines in the mountains. *Arch. Met. Geoph. Biokl.* B **7**, 84–85 (in German).

Dong, Y. Y. & Hallett, J. 1989 Droplet accretion during rime growth and the formation of secondary ice crystals. *Q. Jl R. Met. Soc.* **115**, 127–142.

Dranevic, E. P. 1971 *Glaze and rime.* Leningrad: Gidrometeorologitsheskoe (in Russian).

Eliasson, A. J. & Thorsteins, E. 1996 Wet snow icing combined with strong wind. In *Proc. 7th Int. Workshop on Atmospheric Icing of Structures*, pp. 131–136.

Fekr, M. R., McClure, G. & Hartmann, D. 1998 Investigation of transmission line failure due to ice shedding effects using dynamic analysis. In *Proc. 8th Int. Workshop on Atmospheric Icing of Structures*, pp. 11–16.

Finstad, K. J. & Makkonen, L. 1996 Improved numerical model for wind turbine icing. In *Proc. 7th Int. Workshop on Atmospheric Icing of Structures*, pp. 373–378.

Finstad, K. J., Fikke, S. M. & Ervik, M. 1988*a* A comprehensive deterministic model for transmission line icing applied to laboratory and field observations. In *Proc. 4th Int. Workshop on Atmospheric Icing of Structures*, pp. 227–231.

Finstad, K. J., Lozowski, E. P. & Gates, E. M. 1988*b* A computational investigation of water droplet trajectories. *J. Atmos. Oceanic Technol.* **5**, 160–170.

Finstad, K. J., Lozowski, E. P. & Makkonen, L. 1988*c* On the median volume diameter approximation for droplet collision efficiency. *J. Atmos. Sci.* **45**, 4008–4012.

Fuchs, W., Lutkebohmert, M. & Schickel, K.-P. 1998 Forecast of icing of structures by use of boundary layer model products. In *Proc. 8th Int. Workshop on Atmospheric Icing of Structures*, pp. 179–183.

Gartzman, L. B. 1987 *Probabilities of ice, wind and temperature loads on electrical transmission lines.* Leningrad: Gidrometeoizdat (in Russian).

Gates, E. M., Narten, R., Lozowski, E. P. & Makkonen, L. 1986 Marine icing and spongy ice. In *Proc. 8th IAHR Symp. on Ice, Iowa City, IA*, vol. 2, pp. 153–163.

Gates, E. M., Liu, A. & Lozowski, E. P. 1987 A stochastic model of atmospheric icing. *J. Glaciol.* **34**, 26–30.

Glukhov, V. G. 1989 *Tall building icing on plain territory of the USSR*. Leningrad: Gidrometeoizdat (in Russian).

Golikova, T. N. 1976 Aerodymamic properties of ice covered cables. *Trudy GGO* **379**, 20–29 (in Russian).

Goodwin III, E. J., Mozer, J. D., Di Gioia Jr, A. M. & Power, B. A. 1983 Predicting ice and snow loads for transmission lines. In *Proc. 1st Int. Workshop on Atmospheric Icing of Structures*, pp. 267–273.

Govoni, J. W. & Ackley, S. F. 1983 Field measurements on combined icing and wind loads on wires. In *Proc. 1st Int. Workshop on Atmospheric Icing of Structures*, pp. 205–213.

Grenier, J. C., Admirat, P. & Maccagnan, M. 1986 Theoretical study of the heat balance during the growth of wet snow sleeves on electrical conductions. In *Proc. 3rd Int. Workshop on Atmospheric Icing of Structures*, pp. 125–130.

Hansman, R. J. & Turnock, S. R. 1988 Investigation of microphysical factors which influence surface roughness during glaze ice accretion. In *Proc. 4th Int. Workshop on Atmospheric Icing of Structures*, pp. 139–146.

Holodov, V. U. & Popov, N. I. 1976 The effect of structural parameters of electric overhead lines on iceloads on cables. *Trudy GGO* **379**, 30–36 (in Russian).

Howe, J. B. 1991 Rotating multicylinder method for the measurement of cloud liquid-water content and droplet size. US Army Cold Regions Research and Engineering Laboratory, report 91-2.

Imai, I. 1953 Studies on ice accretion. *Res. Snow Ice* **1**, 35–44 (in Japanese).

Jamaleddine, A., Beauchemin, R., Rousselet, J. & McClure, G. 1996 Weight-dropping simulation of ice-shedding effects on an overhead transmission line model. In *Proc. 7th Int. Workshop on Atmospheric Icing of Structures*, pp. 44–48.

Jones, K. F. 1990 The density of natural ice accretions related to non-dimensional icing parameters. *Q. Jl R. Met. Soc.* **119**, 599–604.

Jones, K. F. & Egelhofer, K. Z. 1991 Computer model of atmospheric ice accretion on transmission lines. US Army Cold Regions Research and Engineering Laboratory, report 91-3.

Knight, C. A. 1968 On the mechansim of spongy hailstone growth. *J. Atmos. Sci.* **25**, 440–444.

Koshenko, A. M. & Bashirova, L. 1979 Recommendations on forecasting the precipitation and deposition (sticking) of wet snow. *Trudy UkrNIGMI* **176**, 96–102 (in Russian).

Kuroiwa, D. 1965 Icing and snow accretion on electric wires. US Army Cold Regions Research and Engineering Laboratory, research report 123.

Laflamme, J. N. & Periard, G. 1996 The climate of freezing rain over the province of Québec in Canada: a preliminary analysis. *Atmos. Res.* **46**, 99–111.

Langmuir, I. & Blodgett, K. B. 1946 A mathematical investigation of water droplet trajectories. In *Collected works of Irving Langmuir*, vol. 10, pp. 335–393. Oxford: Pergamon.

Lehtonen, P., Ahti, K. & Makkonen, L. 1986 The growth and disappearance of iceloads on a tall mast. In *Proc. 3rd Int. Workshop on Atmospheric Icing of Structures*, pp. 363–368.

Lenhard, R. W. 1955 An indirect method for estimating the weight of glaze on wires. *Bull. Am. Meteor. Soc.* **36**, 1–5.

Lesins, G. B., List, R. & Joe, P. I. 1980 Ice accretions. Part I. Testing of new atmospheric icing concepts. *J. Rech. Atmos.* **14**, 347–356.

Levi, L., Nasello, O. B. & Prodi, F. 1991 Morphology and density of ice accreted on cylindrical collectors at low valves of impaction parameter. I. Fixed deposits. *Q. Jl R. Met. Soc.* **117**, 761–782.

PHILOSOPHICAL TRANSACTIONS OF THE ROYAL SOCIETY A MATHEMATICAL, PHYSICAL & ENGINEERING SCIENCES

List, R. 1977 Ice accretion on structures. *J. Glaciol.* **19**, 451–465.

Lock, G. S. H. 1990 *The growth and decay of ice.* Cambridge University Press.

Lock, G. S. H. & Foster, I. B. 1990 Experiments on the growth of spongy ice near a stagnant point. *J. Glaciol.* **36**, 143–150.

Lozowski, E. P., Stallabrass, J. R. & Hearty, P. F. 1983 The icing of an unheated, nonrotationg cylinder. Part I. A simulation model. *J. Climate Appl. Meteor.* **22**, 2053–2062.

Lozowski, E. P., Gates, E. M. & Makkonen, L. 1987 Recent progress in the incorporation of convective heat transfer into cylindrical ice accretion models. In *Proc. Int. Symp. on Cold Regions Heat Transfer, Edmonton, Canada*, pp. 17–24.

Lu, M. L., Popplewell, N., Shah, A. H., Barrett, W. & Au, A. 1998 Mass of ice accretion from freezing rain simulations. In *Proc. 8th Int. Workshop on Atmospheric Icing of Structures*, pp. 89–94.

Ludlam, F. H. 1951 The heat economy of a rimed cylinder. *Q. Jl R. Met. Soc.* **77**, 663–666.

MacArthur, C. D. 1983 Numerical simulation of airfoil ice. In *Proc. 21st Aerospace Sciences Meeting, Reno, NV*, paper AIAA-83-0112.

McComber, P. 1984 Numerical simulation of cable twisting due to icing. *Cold Regions Sci. Technol.* **8**, 253–259.

McComber, P. 1990 Effects of cable twisting on atmospheric ice shedding. In *Proc. 5th Int. Workshop on Atmospheric Icing of Structures*, paper A2-8.

McComber, P. & Bouchard, G. 1986. The numerical calculation of the wind force on two dimensional iced structures. In *Proc. 3rd Int. Workshop on Atmospheric Icing of Structures*, pp. 353–361.

McComber, P. & Touzot, G. 1981 Calculation of the impingement of cloud droplets on a cylinder by the finite element method. *J. Atmos. Sci.* **38**, 1027–1036.

McComber, P., Druez, J. & Savadjiev, K. 1995 Cable twisting due to atmospheric icing. In *Proc. 5th Int. Offhore and Polar Engineering Conf., The Hague*, pp. 461–468.

McKay, G. A. & Thompson, H. A. 1969 Estimating the hazard of ice accretion in Canada from climatological data. *J. Appl. Meteor.* **8**, 927–935.

Macklin, W. C. 1961 Accretion in mixed clouds. *Q. Jl R. Met. Soc.* **87**, 413–424.

Macklin, W. C. 1962 The density and structure of ice formed by accretion. *Q. Jl R. Met. Soc.* **88**, 30–50.

Macklin, W. C. & Bailey, I. H. 1968 The collection efficiency of hailstones. *Q. Jl R. Met. Soc.* **94**, 393–396.

Macklin, W. C. & Payne, G. S. 1968 Some aspects of the accretion process. *Q. Jl R. Met. Soc.* **94**, 167–175.

Macklin, W. C. & Payne, G. S. 1969 The spreading of accreted drops. *Q. Jl R. Met. Soc.* **95**, 724–731.

Maeno, N. & Takahashi, T. 1984 Studies on icicles. I. General aspects of the structure and growth of an icicle. *Low Temp. Sci.* A **43**, 125–138 (in Japanese).

Maeno, N., Makkonen, L., Nishimura, K., Kosugi, K. & Takahashi, T. 1994 Growth rate of icicles. *J. Glaciol.* **40**, 319–326.

Makkonen, L. 1981 Estimating intensity of atmospheric ice accretion on stationary structures. *J. Appl. Meteor.* **20**, 595–600.

Makkonen, L. 1984*a* Atmospheric icing on sea structures. US Army Cold Regions Research and Engineering Laboratory, monograph 84-2, 102, pp. 26–27.

Makkonen, L. 1984*b* Modelling of ice accretion on wires. *J. Climate Appl. Meteor.* **23**, 929–939.

Makkonen, L. 1985 Heat transfer and icing of a rough cylinder. *Cold Regions Sci. Technol.* **10**, 105–116.

Makkonen, L. 1986 The effect of conductor diameter on iceload as determined by a numerical icing model. In *Proc. 3rd Int. Workshop on Atmospheric Icing of Structures*, pp. 81–89.

PHILOSOPHICAL TRANSACTIONS OF THE ROYAL SOCIETY A MATHEMATICAL, PHYSICAL & ENGINEERING SCIENCES

Makkonen, L. 1987 Salinity and growth rate of ice formed by sea spray. *Cold Regions Sci. Technol.* **14**, 163–171.

Makkonen, L. 1988 A model of icicle growth. *J. Glaciol.* **34**, 64–70.

Makkonen, L. 1989 Estimation of wet snow accretion on structures. *Cold Regions Sci. Technol.* **17**, 83–88.

Makkonen, L. 1990 The origin of spongy ice. In *Proc. 10th IAHR Symp. on Ice, Espoo, Finland*, vol. 2, pp. 1022–1030.

Makkonen, L. 1992 Analysis of rotating multicylinder data in measuring cloud droplet size and liquid water content. *J. Atmos. Oceanic Technol.* **9**, 258–263.

Makkonen, L. 1998 Modeling power line icing in freezing precipitation. *Atmos. Res.* **46**, 131–142.

Makkonen, L. & Fujii, Y. 1993 Spacing of icicles. *Cold Regions Sci. Technol.* **21**, 317–322.

Makkonen, L. & Oleskiw, M. 1997 Small-scale experiments on rime icing. *Cold Regions Sci. Technol.* **25**, 173–182.

Makkonen, L. & Stallabrass, J. R. 1984 Ice accretion on cylinders and wires. National Research Council of Canada, NRC, technical report TR-LT-005.

Makkonen, L. & Stallabrass, J. R. 1987 Experiments on the cloud droplet collision efficiency of cylinders. *J. Climate Appl. Meteor.* **26**, 1406–1411.

Marjaniemi, M. & Peltola, E. 1996 A blade heating element design method. In *Proc. Wind Energy Production in Cold Climates, BOREAS III*, pp. 340–354. Finnish Meteorological Institute.

Matsuo, T. & Sasyo, Y. 1981 Melting of snowflakes below freezing level in the atmosphere. *J. Meteor. Soc. Japan* **59**, 10–26.

Mazin, I. P. 1957 *Physical principles of aircraft icing.* Leningrad: Gidrometeoizdat (in Russian).

Messinger, B. L. 1953 Equilibrium temperature of an unheated icing surface as a function of air speed. *J. Aeronaut. Sci.* **20**, 29–42.

Mulherin, N. D. 1998 Atmospheric icing and communication tower failure in the United States. *Cold Regions Sci. Technol.* **27**, 91–104.

Nikiforov, E. P. 1983 Icing related problems, effect of line design and iceload mapping. In *Proc. 1st Int. Workshop on Atmospheric Icing of Structures*, pp. 239–245.

Oleskiw, M. M. & Lozowski, E. P. 1983 The design and testing of a Lagrangian computer model for simulating time-dependent rime icing on two-dimensional structures. In *Proc. 1st Int. Workshop on Atmospheric Icing of Structures*, pp. 59–66.

Olsen, W. & Walker, E. 1986 Experimental evidence for modifying the current physical model for ice accretion on aircraft surfaces. In *Proc. 3rd Int. Workshop on Atmospheric Icing of Structures*, pp. 193–250.

Personne, P. & Duroure, C. 1987 Modeling of the structure of soft rime. *J. Physique* C **1**, 413–449 (in French).

Personne, P. & Gayet, J.-F. 1988 Ice accretion on wires and anti-icing induced by Joule effect. *J. Appl. Meteor.* **27**, 101–114.

Personne, P., Duroure, C. & Gayet, J.-F. 1988 Effect of the surface roughness on the iceload characteristics during icing with low airspeeds. In *Proc. 4th Int. Workshop on Atmospheric Icing of Structures*, pp. 232–235.

Personne, P., Duroure, C. & Isaka, H. 1990 Theoretical study of air inclusions on rotating cylinders. In *Proc. 5th Int. Workshop on Atmospheric Icing of Structures*, paper A2-6.

Phan, C. L. & Laforte, J.-L. 1981 The influence of electro-freezing on ice formation on high-voltage dc transmission lines. *Cold Regions Sci. Technol.* **4**, 15–25.

Poots, G. 1996 *Ice and snow accretion on structures.* Taunton: Research Studies Press.

Poots, G. 1998 Aspects of a model for wet-snow accretion on an overhead line conductor. In *Proc. 8th Int. Workshop on Atmospheric Icing of Structures*, pp.185–189.

Poots, G. & Rodgers, G. G. 1976 The icing of a cable. *J. Inst. Math. Applic.* **18**, 203–217.

PHILOSOPHICAL TRANSACTIONS OF THE ROYAL SOCIETY A MATHEMATICAL, PHYSICAL & ENGINEERING SCIENCES

Poots, G. & Skelton, P. L. I. 1995 Simulation of wet-snow accretion by axial growth on a transmission line. *Appl. Math. Modelling* **19**, 514–517.

Porcu, F., Smargiassi, E. & Prodi, F. 1995 2-D and 3-D modelling of low density ice accretion on rotating wires with variable surface irregularities. *Atmos. Res.* **36**, 233–242.

Reisner, J., Ramussen, R. M. & Bruintjes, R. T. 1998 Explicit forecasting of supercooled liquid water in winter storms using the MM5 mesoscale model. *Q. Jl R. Met. Soc.* **124**, 1071–1107.

Rink, J. 1938 The melt water equivalent of rime deposits. In *Reichsamt fur Wetterdienst, Wissenschaftliche Abhandlungen*, vol. 5 (in German).

Rogers, D. C., Baumgartner, D. & Vali, G. 1983 Determination of supercooled liquid water content by measuring rime rate. *J. Climate Appl. Meteor.* **22**, 153–162.

Sakamoto, Y. & Ishihara, K. 1984 An estimating method of snow load on overhead power lines. In *Proc. 2nd Int. Workshop on Atmospheric Icing of Structures*, pp. 137–140.

Sakamoto, Y. & Miura, A. 1993 Comparative study of wet snow models for estimating snow load on power lines based on general meteorological parameters. In *Proc. 6th Int. Workshop on Atmospheric Icing of Structures*, pp. 133–138.

Scavuzzo, R. J., Chu, M. L. & Ananthaswamy, V. 1994 Influence of aerodynamic forces in ice shedding. *J. Aircraft* **31**, 526–530.

Schlichting, H. 1979 *Boundary-layer theory.* McGraw-Hill

Scott, J. N., Hankey, W. L., Giessler, F. J. & Gielda, T. P. 1987 Navier–Stokes solution to the flowfield over ice accretion shapes. *J. Aircraft* **25**, 710–716.

Shin, J., Berkowitz, B., Ghen, H. H. & Cebeci, T. 1994 Prediction of ice shapes and their effect on airfoil drag. *J. Aircraft* **31**, 263–270.

Skelton, P. L. I. & Poots, G. 1991 Snow accretion on overhead line conductors of finite torsional stiffness. *Cold Regions Sci. Technol.* **19**, 301–316.

Snitkovskii, A. I. 1977 Prediction of dangerous weather phenomena and prospects for research in this area. *Sov. Meteor. Hydrol.* **11**, 71–80.

Stallabrass, J. R. 1983 Aspects of freezing rain simulation and testing. In *Proc. 1st Int. Workshop on Atmospheric Icing of Structures*. pp. 67–74.

Sundin, E. & Makkonen, L. 1998 Ice loads on a lattice tower estimated by weather station data. *J. Appl. Meteor.* **37**, 523–529.

Szilder, K. 1993 The density and structure of ice accretion predicted by a random walk model. *Q. Jl R. Met. Soc.* **119**, 907–924.

Szilder, K. & Lozowski, E. P. 1994 An analytical model of icicle growth. *Ann. Glaciol.* **19**, 141–145.

Szilder, K. & Lozowski, E. P. 1995*a* A new method of modelling ice accretion on objects of complex geometry. *Int. J. Offshore Polar Engng* **5**, 37–42.

Szilder, K. & Lozowski, E. P. 1995*b* Simulation of icicle growth using a three-dimensional random walk model. *Atmos. Res.* **36**, 243–249.

Szilder, K. & Lozowski, E. P. 1996 Three-dimensional modelling of ice accretion microstructure. In *Proc. 7th Int. Workshop on Atmospheric Icing of Structures*, pp. 60–63.

Szilder, K., Lozowski, E. P. & Gates, E. M. 1987 Modelling ice accretion on non-rotating cylinders—the incorporation of time dependence and internal heat conduction. *Cold Regions Sci. Technol.* **13**, 177–191.

Vassbø, T., Kristjansson, J. E., Fikke, F. M. & Makkonen, L. 1998 An investigation of the feasibility of predicting icing episodes using numerical weather prediction model output. In *Proc. 8th Int. Workshop on Atmospheric Icing of Structures*, pp. 343–347.

Waibel, K. 1955 Meteorological conditions of rime deposition on high voltage lines in the mountains. *Arch. Met. Geoph. Biokl.* B **7**, 74–83 (in German).

Wakahama, G., Kuroiwa, D. & Goto, D. 1977 Snow accretion on electric wires and its prevention. *J. Glaciol.* **19**, 479–487.

Yano, K. 1988 Studies of icing and ice-snow accretion in Mt Zao. In *Proc. 4th Int. Workshop on Atmospheric Icing of Structures*, pp. 109–113.

Zavarina, M. V., Glukhov, V. G. & Mytariev, M. N. 1976 A method for the calculation of iceloads on high constructions. *Zeitsch. Meteor.* **26**, 98–104 (in German).

Zerr, R. J. 1997 Freezing rain: an observational and theoretical study. *J. Appl. Meteor.* **36**, 1647–1661.